Available online at www.sciencedirect.com
ScienceDirect
Journal of Power Sources 180 (2008) 546–552
JOURNAL OF POWER SOURCES
www.elsevier.com/locate/jpowsour

Amphoteric effects of Fe_2P on electrochemical performance of lithium iron phosphate–carbon composite synthesized by ball-milling and microwave heating

Min-Sang Song [a], Dong-Yung Kim [a], Yong-Mook Kang [b], Yong-Il Kim [c], Jai-Young Lee [d], Hyuk-Sang Kwon [a,*]

[a] *Department of Materials Science and Engineering, Korea Advanced Institute of Science and Technology, 373-1 Guseong-Dong, Yuseong-gu, Daejeon, Republic of Korea*
[b] *Division of Advanced Materials Engineering, Kongju National University, 275 Budae-dong, Cheonan, Chungnam, Republic of Korea*
[c] *Korea Research Institute of Standards and Science, P.O. Box 102, Yuseong, Daejeon, Republic of Korea*
[d] *INVEST & Department of Advanced Technology Fusion, Konkuk University, 1 Hwayang-dong, Gwangjin-Gu, Seoul, Republic of Korea*

Received 21 October 2007; received in revised form 6 January 2008; accepted 20 January 2008
Available online 14 February 2008

Abstract

Lithium iron phosphate–carbon ($LiFePO_4$–C) composites with various amounts of Fe_2P are synthesized by ball-milling coupled with microwave heating to serve as cathodes for lithium-ion batteries. $LiFePO_4$–C in which Fe_2P is restrained below a critical concentration gives as very high discharge capacity of 165 mAh g^{-1}, excellent rate capability (85.4% *C*/50-rate discharge capacity at 2*C*) and stable cyclic retention for 250 cycles. Above the critical concentration however, electrochemical performance deterioated. Analysis and debate, based on a comparison of the physical and electrochemical properties among $LiFePO_4$–C composites with the variation of Fe_2P, proceeded to the conclusion that below the critical concentration, Fe_2P enhanced the conductivity of $LiFePO_4$–C, whereas above the critical concentration, it blocked the one-dimensional Li^+ pathways in $LiFePO_4$ and might hinder Li^+ movement in $LiFePO_4$. Therefore, in order to obtain a $LiFePO_4$–C composite that enhances electrochemical performance, it is concluded that the amount of Fe_2P should be carefully controlled below its critical concentration.

Keywords: Lithium iron phosphate–carbon composites; Discharge capacity; Rate capability; Cyclic retention; Critical concentration; Lithium-ion battery

1. Introduction

Lithium-ion batteries, in which graphite and $LiCoO_2$ are employed as the electrode materials, are widely used as a power source for most portable electronic devices such as cellular phones, camcorders, digital cameras and laptop computers due to their high specific energy and excellent cycle performance. The successful application of $LiCoO_2$ as the commercial cathode material for Li-ion batteries is attributed to its high Li-ion and electron conductivity, high potential vs. Li^+/Li (∼4 V), excellent capacity retention during cycling, and a practical capacity of about 140 mAh g^{-1} [1]. On the other hand, its poor thermal stability and high cost have prevented $LiCoO_2$ from being used for large-scale Li-ion batteries, which are required for novel appliances such as hybrid electric vehicles (HEVs), electric vehicles (EVs), e-bikes and robot cleaners [2–5]. Therefore, there is an apparent need to develop a new cathode material with excellent thermal stability and low cost.

Because an olivine-structured material, $LiFePO_4$, features excellent thermal stability, low cost and high reversibility in Li^+ insertion/extraction, it has been considered as the most promising cathode material for the large-scale Li-ion batteries [6–10]. Nevertheless, its low electronic and ionic conductivity [11,12], and some difficulties in synthesizing single-phase material [9,13] have hindered the practical application of $LiFePO_4$ as a cathode material. Therefore, new strategies have been attempted for improving the electronic and ionic conductivity of $LiFePO_4$ such as carbon coating [14–19], particle size reduction [12,13,20] and supervalent cation doping [21]. In addition, various methods such as solid-state reac-

* Corresponding author. Tel.: +82 42 869 3326; fax: +82 42 869 3310.
E-mail address: hskwon@kaist.ac.kr (H.-S. Kwon).

0378-7753/$ – see front matter © 2008 Elsevier B.V. All rights reserved.
doi:10.1016/j.jpowsour.2008.01.079

tion, mechanochemical activation, sol–gel route, hydrothermal reaction and co-precipitation [12–21] have been introduced to synthesize single-phase $LiFePO_4$ since Padhi et al. [6,7] reported the feasibility of $LiFePO_4$ as a cathode material. Among these strategies, carbon coating coupled with a reduction in the particle size of $LiFePO_4$ to yield a lithium iron phosphate–carbon ($LiFePO_4$–C) composite has been generally tried because it enhances both the electronic and the ionic conductivity of $LiFePO_4$ [14–19]. At this stage, however, various routes for synthesizing effective $LiFePO_4$–C composites are still under development.

Microwave heating is a very powerful and efficient synthetic method in which the target materials can be obtained in a short time at low temperature (typically 100–200 °C below the temperature involved in conventional furnace heating) [22]. We have succeeded in simply and rapidly synthesizing $LiFePO_4$–C by microwave heating accompanied with vibrant ball-milling [23]. It was observed that Fe_2P, evolved by breakage of the covalent bond between phosphorus and oxygen in the PO_4^{3-} polyanion and bond formation between iron and phosphorus, exists in the $LiFePO_4$–C composite when the microwave heating time is beyond a critical time [13].

In the early stage of $LiFePO_4$ research, Fe_2P was considered as a by-product that should be excluded during synthesis of single-phase $LiFePO_4$, as pointed out by Arnold et al. [13]. By contrast, Herle et al. [24] demonstrated that metal phosphocarbides and Fe_2P (metallic compound, σ: 10^{-1} S cm^{-1} at room temperature) play a crucial role in enhancing the electronic conductivity of $LiFePO_4$–C composite up to $\sim 10^{-2}$ S cm^{-1}. Based on this work, it appears that the conductivity enhancement by Fe_2P may contribute to the improvement in the rate capability of the $LiFePO_4$–C composite. The above authors did not, however, confirm a positive effect of Fe_2P on the electrochemical performance of the $LiFePO_4$–C composite. Aside from this report, there has not been any systematic research to clarify the correlation between the existence of Fe_2P and the electrochemical performance of $LiFePO_4$–C composite.

In the study reported here, the amphoteric effect of Fe_2P on the electrochemical performance of $LiFePO_4$–C composite is clarified based on structural and electrochemical observations.

2. Experimental

2.1. Preparation of synthesis

$LiFePO_4$–C was prepared by ball-milling and microwave heating method using Li_3PO_4 (Aldrich) and $Fe_3(PO_4)_2{\cdot}8H_2O$ (Kojundo) as the precursor materials. Full details of the preparation route have been reported in the previous publication [23].

2.2. Characterization of material

In order to confirm the phase of the $LiFePO_4$–C, XRD analysis (D/max-IIIC, Rigaku) was conducted from 15° to 45° at a scan rate of 1° min^{-1} using Cu Kα radiation. The morphology of $LiFePO_4$–C was observed by TEM (transmission electron microscopy, JEOL) operating at 300 kV, and the particle size of $LiFePO_4$–C was measured by a LPSA (laser particle size analyzer, LS230 System/Small Volume Module, Beckman Coulter) equipped with a polarization intensity differential scattering (PIDS) analyzer and a 116-channel detector for detecting 0.4–0.04 μm sized particles. The amount of residual carbon in $LiFePO_4$–C was measured by means of a CHNS elemental analyzer (Vario EL III, Elementar). The room temperature conductivity was measured on microwave-sintered pellets (∼12.5 mm diameter and ∼1 mm thickness) by four-point dc methods (SR1000, Chang-Min Co.). A two-phase Rietveld refinement was performed for more sensitive detection of Fe_2P using the GSAS (general structure analysis system) program [25]. The XRD data for Rietveld refinement were measured from 15° to 120° at a step of 0.02° using Cu Kα radiation with a graphite monochromator in the reflection geometry (Dmax2200V, Rigaku). Silicon (NIST 640c) powder was chosen as an external standard to correct the zero-point shift for the measured diffraction data. Mössbauer spectroscopy (MR351, FAST) with ^{57}Co γ-ray source was also employed for accurately detecting Fe_2P in $LiFePO_4$–C. Velocity calibration was carried out using the spectrum of α-Fe at room temperature.

2.3. Cell fabrication and electrochemical analysis

The slurry for the $LiFePO_4$–C cathode was prepared by mixing $LiFePO_4$–C and acetylene black, to which was added a *N*-methyl-2-pyrrolidene (NMP) solution containing polyvinylidene fluoride (PVdF). The weight ratio (wt.%) of $LiFePO_4$, acetylene black (residual amount in $LiFePO_4$–C and mixed amount) and PVdF was 72:20:8. The slurries were coated on Al foil substrates by baker applicator (Yoshimitsu) to give a uniform thickness, and then dried for 12 h at 120 °C in a vacuum oven. The dried cathodes were pressed and then cut into a 1.33 cm^2 discs. The cathode (except Al foil) mass and thickness were ∼5.5 mg cm^{-2} and ∼50 μm, respectively. 2016 coin-type cells (Toyo system) were assembled in an argon-filled glove box (M-braun MB 20G) by placing a microporous polypropylene separator (Celgard 2400^{TM}) between the cathode and the lithium metal foil anode (Cyprus Foote Mineral, 99.98%, USA). A constant volume (120 μl) of liquid electrolyte (1 M $LiClO_4$ in 1:1 ethylene carbonate/dimethyl carbonate (EC/DMC; (Merck)) was added to the cell during cell fabrication. The cells were charged and discharged galvanostatically between 2.5 and 4.3 V (vs. Li/Li$^+$) using a Toscat-3100u battery tester (Toyo System). The rest time between charging and discharging was 10 min. Various charge–discharge rates (C-rates) based on the nominal capacity measured at a extremely low rate were applied to examine the rate capability of $LiFePO_4$–C.

3. Results and discussion

Fig. 1 shows XRD patterns of a $LiFePO_4$–C composite prepared by ball-milling for 30 min and subsequent microwave heating for 2–4 min, respectively. For the sample microwave heated for 2 min, all of the peaks in the XRD pattern are assigned to the triphylite $LiFePO_4$. After microwave heating for 3 min, an additional peak corresponding to the Fe_2P phase appears.

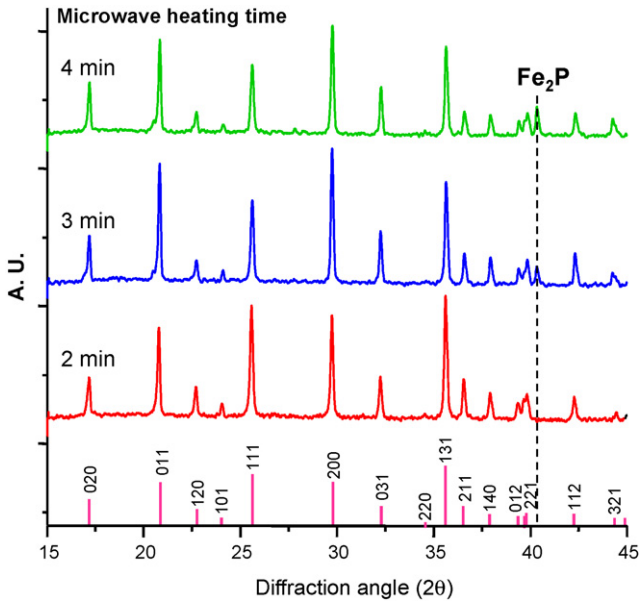

Fig. 1. X-ray diffraction patterns of $LiFePO_4$–C prepared by ball-milling for 30 min and subsequent microwave heating for 2–4 min, and inorganic crystal structure database (ICSD) reference pattern (no. 83-2092; triphylite $LiFePO_4$) in JADE5 software.

This means that the atmosphere encompassing the precursors of $LiFePO_4$ was sufficiently reductive to form Fe_2P. Hence, a microwave heating time above 4 min increases the amount of Fe_2P phase, as confirmed by the increase in the Fe_2P peak intensity in the XRD pattern.

In Fig. 2, the TEM images of $LiFePO_4$–C are given with the selected area diffraction patterns (SADP). As shown in the TEM images, $LiFePO_4$–C composites have similar morphologies ($LiFePO_4$ particle size, degree of carbon distribution), irrespective of the heating time. Two distinctive forms of particles (polygonal particles and cotton-like particles) are observed in the TEM images; each is identified as crystalline $LiFePO_4$ and amorphous carbon. This SADP also reveals that the $LiFePO_4$ particle is characteristic of a single crystal. In the $LiFePO_4$–C composite, most of $LiFePO_4$ particles are connected by amorphous carbon, and $LiFePO_4$ is uniformly distributed with carbon.

The results from laser particle size analysis and elemental analysis of the $LiFePO_4$–C composite are summarized in Table 1. From the mean particle size, D75 and D90 in Table 1, it is concluded that the $LiFePO_4$–C composite has small particle size and a homogeneous size distribution. The increase in particle size with variation in the microwave heating time is very slight, as expected from the study by Nakayama et al. [26]. Because microwave heating can minimize undesirable grain growth without any grain-growth inhibitors [22], it appears that the $LiFePO_4$–C composite maintains a grain size similar to that of the initial grain. Another reason for the restrained grain growth of $LiFePO_4$ is that the uniform distribution of carbon around $LiFePO_4$ hinders grain growth [27].

In Table 1, the continuous decrease in residual carbon content (from an initial 5 wt.% to a final 2.874 wt.%) with microwave heating time implies that more carbon is oxidized to CO_2 or CO gas (carbothermal reaction) with longer microwave heating. For furnace heating, a decrease in the amount of carbon acting as a grain-growth inhibitor gives rise to a substantial increase in $LiFePO_4$ grain size [27]. As for microwave heating, a decrease in the carbon content has little influence on the grain growth of $LiFePO_4$.

The initial charge–discharge curves of the $LiFePO_4$–C composite are presented in Fig. 3a. In the discharge curve for the $LiFePO_4$–C composite prepared by microwave heating for 2 min, a long and flat voltage-plateau appears at around 3.41 V, and then the voltage falls sharply to the cut-off value (2.5 V). This behaviour yields a high discharge capacity of 165 mAh g^{-1} (97.1% of the theoretical capacity of $LiFePO_4$). For Fe_2P-included $LiFePO_4$–C composites produced by microwave heating for 3 and 4 min, shorter voltage-plateaux appear, and then the voltage drops gradually to give low discharge capacities of 111 and 97 mAh g^{-1}, respectively. Given that the amount of Fe_2P in the Fe_2P-included $LiFePO_4$–C composite is small, as predicted by the low peak intensity in Fig. 1, it appears that the significant reduction in the charge–discharge capacity of the Fe_2P-included $LiFePO_4$–C composite is not primarily related to the amount of electrochemically inactive Fe_2P.

From Fig. 3b, it can be seen that the $LiFePO_4$–C composite produced by microwave heating for 2 min provides an excellent rate capability that maintains 85.4% of the *C*/50-rate discharge capacity at 2*C*, but the other composites obtained by microwave heating for 3 and 4 min sustain only 65.5% and 47.8%, respectively. In addition, the $LiFePO_4$–C composite synthesized by

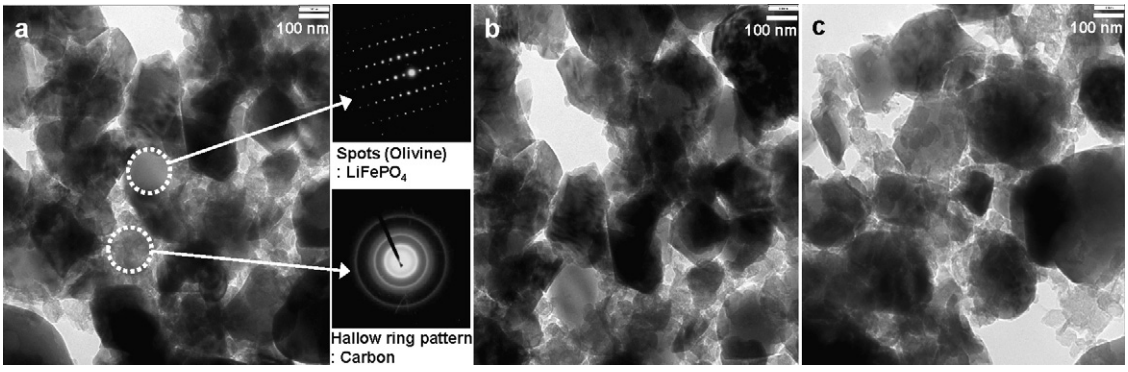

Fig. 2. TEM images of $LiFePO_4$–C prepared by ball-milling for 30 min and microwave heating for (a) 2 min, (b) 3 min and (c) 4 min, and selected area diffraction pattern (SADP).

Table 1
Particle size of $LiFePO_4$–C measured by LPSA and carbon content (wt.%) in $LiFePO_4$–C detected by CHNS elemental analyzer

Microwave heating time (min)	Mean particle size (μm)	*D*25 (μm)	*D*50 (μm)	*D*75 (μm)	*D*90 (μm)	Carbon content (wt.%)
2	0.530	0.157	0.365	0.522	1.590	3.817
3	0.585	0.123	0.280	0.526	1.851	3.299
4	0.640	0.145	0.322	0.592	1.903	2.874

Particle size *Dn*: *D* is particle diameter and *n* is cumulative percentage in volume distribution. Given the group of particles cumulated up to *n* percent, *Dn* signifies the diameter of the largest particle in that group.

microwave heating for 2 min has an outstanding rate capability, its capacity at 30*C* corresponds to 58.9% (97 mAh g^{-1}) of the discharge capacity at *C*/50, as illustrated in Fig. 3c. Based on the previous result that the conductivity of $LiFePO_4$–C composite can be enhanced by Fe_2P [24], it is contradictory that the rate capability of $LiFePO_4$–C composite including Fe_2P is much inferior to that of $LiFePO_4$–C composite excluding Fe_2P. Moreover, four-point dc conductivity measurement show that the $LiFePO_4$–C composites prepared by microwave heating have the similar conductivities, irrespective of the heating time; 1.00×10^{-1} S cm^{-1} for 2 min, 1.06×10^{-1} S cm^{-1} for 3 min, and 1.15×10^{-1} S cm^{-1} for 4 min. Therefore, the inferior rate capability of Fe_2P-included $LiFePO_4$–C seems to result from not the variation in the amount of carbon or the morphological difference but from other factors that accompany the formation of Fe_2P.

It is well known that when the cell reaction rate is forced to increase for supplying higher current to an external circuit, the poor reaction kinetics decrease the cell capacity by dropping the cell voltage faster. Therefore, the decrease in the capacity of Fe_2P-included $LiFePO_4$–C composite, shown in Fig. 3a, may be associated with its poor rate capability in Fig. 3b. In fact, the discharge capacity of the Fe_2P-included $LiFePO_4$–C composite increases with reducing the discharging rate below *C*/50 (1*C* = 170 mA g^{-1}), then eventually approaches the nominal discharge capacity (113 mAh g^{-1} for the 3 min-microwave heated $LiFePO_4$–C, 99 mAh g^{-1} for the 4 min-microwave heated $LiFePO_4$–C). Considering the discharge capacity at *C*/50 in Fig. 3a, however, the increment in discharge capacity is relatively small. Therefore, the poor rate capability of the Fe_2P-included $LiFePO_4$–C composite hardly affects the decrease in its discharge capacity shown in Fig. 3a. This means that the decrease in the capacity in Fig. 3a also has no significant relation to the poor rate capability.

As mentioned above, the $LiFePO_4$–C composite prepared in this work has an electronic conductivity in the range of $1.00–1.15 \times 10^{-1}$ S cm^{-1} depending on the microwave heating time. These values almost reach the most enhanced conductivities observed by Herle et al. [24]. This suggests that the Fe_2P phase may also be formed in the $LiFePO_4$–C composite prepared by 2 min-microwave heating, because the conductivity of the $LiFePO_4$–C composite cannot reach about 10^{-1} S cm^{-1} at room temperature without Fe_2P, as reported by Xu et al. [27]. Yamada et al. [9] demonstrated that small amount of impurities were not detected by XRD analysis. Therefore, it was clear that more sensitive detection tools are required to confirm the presence of Fe_2P.

Fig. 4a and b shows the results from studies with X-ray Rietveld refinement and Mössbauer spectroscopy, respectively. The two-phase X-ray Rietveld refinement reveals that 0.56 wt.% Fe_2P is present in the $LiFePO_4$–C composite synthesized by 2 min-microwave heating. Mössbauer spectroscopy also supports the existence of Fe_2P, as shown in Fig. 4b. The amount of Fe_2P detected by Mössbauer spectroscopy is 1.03 wt.% in the $LiFePO_4$–C composite produced by 2 min-heating and 14.15 wt.% in case of 4 min-heating. Mössbauer spectroscopy is a very useful tool to detect the impurity phases because it can catch non-crystalline as well as crystalline phases in contrast to the X-ray diffraction that detects only crystalline phases [29]. The complementary use of X-ray Rietveld refinement and Mössbauer spectroscopy allows confirmation of the formation of Fe_2P. As a result, it is clarified that the excellent electrochemical performance of $LiFePO_4$–C prepared by 2 min-microwave heating comes not only from the good crystallinity, small particle size and extremely uniform carbon distribution, but also from enhancement of the electronic conductivity by Fe_2P.

Fig. 5 shows the excellent cycle performance of the $LiFePO_4$–C composite synthesized by 2 min-microwave heating, where the initial discharge capacity (148 mAh g^{-1}) obtained at *C*/2 is maintained up to the 250th cycle. By contrast, the $LiFePO_4$–C composites synthesized by microwave heating for 3 and 4 min exhibit poor cycle behaviour, even at *C*/10. These trends in cycling capability are consistent with those observed for charge–discharge capacity and rate capability.

The aim of this work is to demonstrate that the electrochemical performance of $LiFePO_4$–C composites clearly depends on the concentration of Fe_2P. Actually, the deteriorated electrochemical properties are obtained above the critical concentration of Fe_2P and vice versa. The positive effect of Fe_2P below the critical concentration can be attributed to increased conductivity of the $LiFePO_4$–C composite caused by Fe_2P, but the reason for the negative effect is not clear. Nevertheless, based on the conclusions from the electrochemical data and the physical properties of $LiFePO_4$–C, it can be inferred that the formation of Fe_2P above the critical concentration leads to disruption of the one-dimensional Li^+ pathways followed by hindrance of Li^+ transport [30].

The disrupting effect is easily verified from the Mössbauer spectroscopy data in Fig. 4b. Based on the amount of Fe_2P detected, the capacity evolved by pure $LiFePO_4$ can be calculated. The nominal discharge capacity evolved by pure $LiFePO_4$ for the $LiFePO_4$–C composite synthesized by 2 min-microwave heating is 167 mAh g^{-1}, while that for the

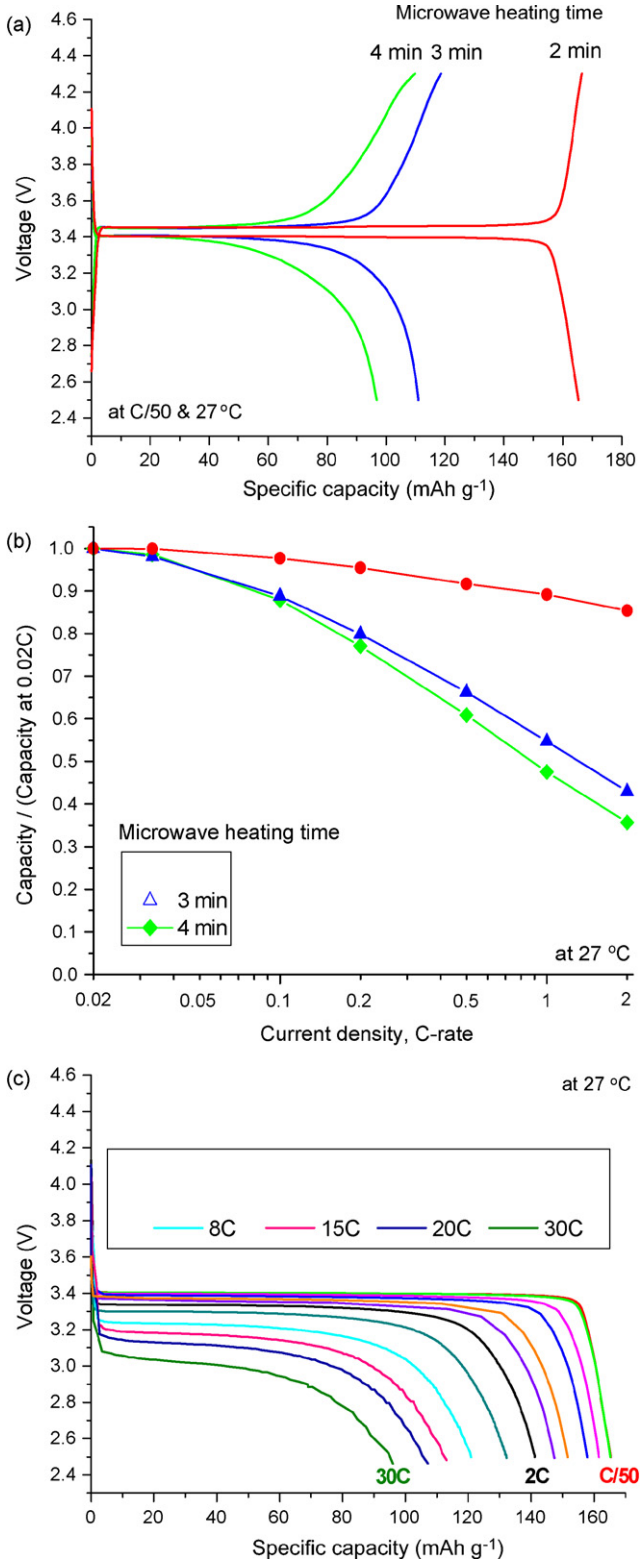

Fig. 3. (a) Galvanostatic charge–discharge curves of $LiFePO_4$–C at 27 °C. *C*/50 rate ($1C = 170\ mA\ g^{-1}$). (b) Rate capability of $LiFePO_4$–C at 27 °C. Various current densities based on nominal capacity (2 min; $165\ mA\ h\ g^{-1}$, 3 min; $113\ mA\ h\ g^{-1}$, 4 min; $99\ mA\ h\ g^{-1}$) measured at extremely low rates of less than *C*/50 used in the test. Current density of each sample is: 2 min; $1C = 165\ mA\ g^{-1}$, 3 min; $1C = 113\ mA\ g^{-1}$, 4 min; $1C = 99\ mA\ g^{-1}$. (c) Discharge curves of $LiFePO_4$–C prepared by 2 min-microwave heating collected at various *C*-rates from *C*/50 to 30*C* ($1C = 165\ mA\ g^{-1}$).

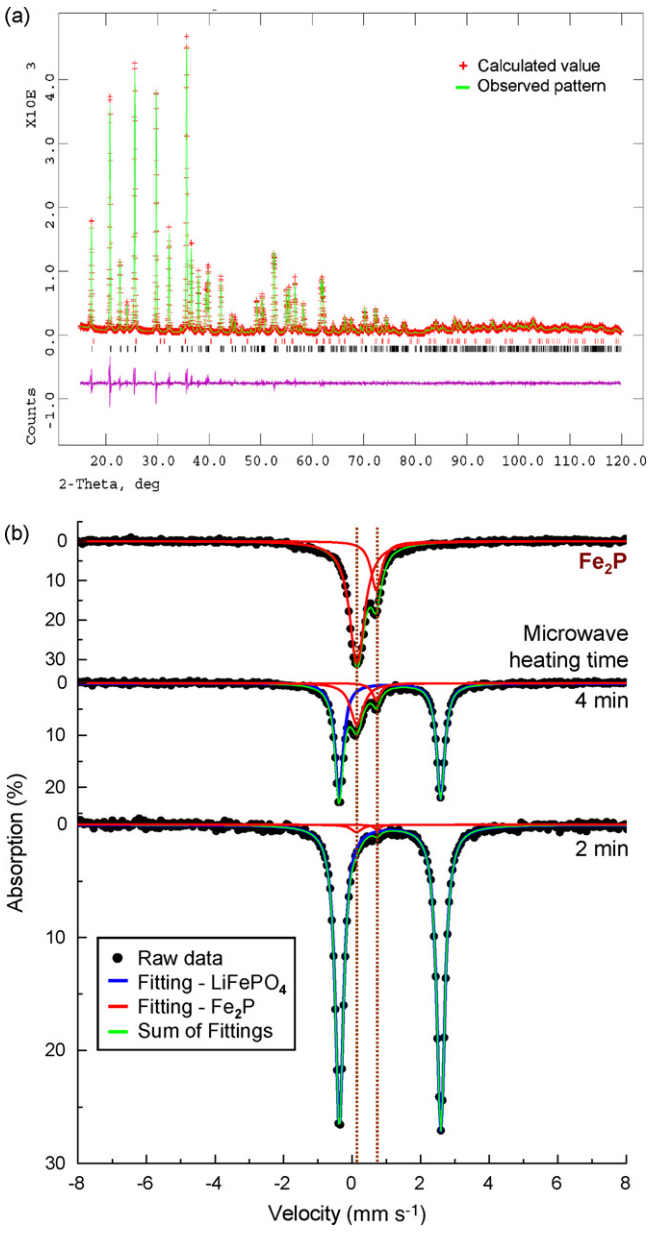

Fig. 4. (a) Rietveld refinement patterns of $LiFePO_4$–C prepared by 2 min-microwave heating. A difference (obs. − cal.) plot is shown beneath. Tick marks above the difference data indicate the reflection position. Upper and lower tick marks above the difference data indicate the reflection position for Fe_2P and $LiFePO_4$ phases, respectively. $R_{wp} = 11.16\%$, $R_p = 8.15$, $\chi^2 = 1.93$, weight fraction (wt.%) of $LiFePO_4$ to $Fe_2P = 99.44{:}0.56$. (b) Mössbauer spectra of pure Fe_2P and $LiFePO_4$–C synthesized by microwave heating for 2 and 4 min. At 2 min-microwave heating, IS (isomer shift) and QS (quadrupole splitting) for blue doublet are 1.11 and $2.96\ mm\ s^{-1}$, respectively. With 4 min-microwave heating, IS and QS for the blue doublet are 1.10 and $2.96\ mm\ s^{-1}$, respectively. These IS values typically correspond to those for Fe^{2+} ion [28]. Comparison of Fe_2P Mössbauer spectrum with other spectra confirms that red peaks originate from Fe_2P. Weight fractions (wt.%) of $LiFePO_4$ to Fe_2P are 98.97:1.03 for 2 min and 85.85:14.15 for 4 min. (For interpretation of the references to color in this figure legend, the reader is referred to the web version of the article.)

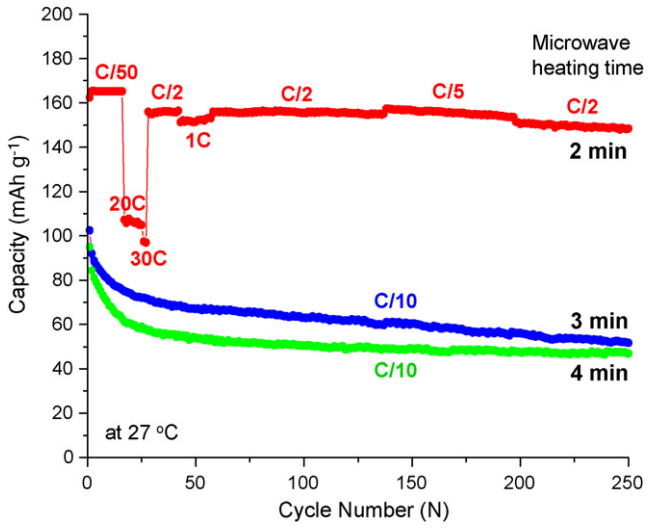

Fig. 5. Cyclic performance of $LiFePO_4$–C at 27 °C. For $LiFePO_4$–C produced by 2 min-microwave heating, the cycling test was carried out by varying the current density.

4 min-microwave heated sample is only 113 mAh g^{-1}. With the latter composite, therefore, the Li^+ pathways in $LiFePO_4$ are blocked, which decreases the intrinsic Li-capacity of $LiFePO_4$. This disrupting effect is the obvious reason for the decrease in the capacity shown in Fig. 3a, but does not explain why the rate capability and the cycle performance are degraded, as seen in Figs. 3b and 5, respectively, because they are associated with Li^+ moving into or out of the $LiFePO_4$ framework for completing the total cell reaction ($Li_{1-x}FePO_4 + xLi^+ + xe^- \rightarrow LiFePO_4$).

From the X-ray diffraction patterns in Fig. 1, it is found that the intensity ratio of peaks of $LiFePO_4$ for the 2 min-microwave heated sample is similar to that of the corresponding peaks in the ICSD pattern. By contrast, the intensity ratio of the peaks of $LiFePO_4$ for the 3 or 4 min-microwave heated samples is different from that of the corresponding peaks in the ICSD pattern. This change in the peak intensity ratio can stem from a chemical inhomogeneity (the change in the atomic arrangements in the $LiFePO_4$ unit cell) [31,32]. Accordingly, Li^+ transport through the one-dimensional Li^+ pathways of $LiFePO_4$ may be hindered by the chemical inhomogeneity above the critical concentration of Fe_2P. If the hindering effect be verified, it can account for the degradation of the rate capability and the cycle performance. Having recognized this clue found in the X-ray diffraction data, we are continuing to study the effects of the formation of Fe_2P on Li^+ motion in $LiFePO_4$ with the intention of elucidating the reason for the hindering effect of Fe_2P.

4. Conclusions

A study has been conducted of the physical and electrochemical properties of $LiFePO_4$–C composites with variation of Fe_2P amount and synthesized by ball-milling followed by microwave heating. $LiFePO_4$–C with Fe_2P formed within the critical concentration delivers a very high discharge capacity, excellent rate capability and stable cycle behaviour. By contrast, $LiFePO_4$–C with Fe_2P formed above the critical concentration gives much poorer electrochemical performance. This phenomenon is because within the critical concentration of Fe_2P, the formation of Fe_2P only increases the conductivity of $LiFePO_4$–C, where as above the critical concentration of Fe_2P, it causes blocking of the one-dimensional Li^+ pathways in $LiFePO_4$ and offers the possibility of hindering Li^+ movement in $LiFePO_4$. Although the in situ formation of Fe_2P in $LiFePO_4$ during the synthesis process is a very promising method to enhance the electrochemical performance of $LiFePO_4$–C. The amount of Fe_2P should be carefully controlled to prevent the negative effect of Fe_2P.

References

[1] M. Wakihara, Mater. Sci. Eng. R 33 (2001) 109.
[2] M. Winter, J.O. Besenhard, M.E. Spahr, P. Novák, Adv. Mater. 10 (1998) 725.
[3] K. Striebel, 11th IMLB, Monterey, CA, June 2002, abstract #125.
[4] D.D. MacNeil, Z. Lu, Z. Chen, J.R. Dahn, J. Power Sources 108 (2002) 8.
[5] J. Jiang, J.R. Dahn, Electrochem. Commun. 6 (2004) 39.
[6] A.K. Padhi, K.S. Nanjundaswamy, J.B. Goodenough, J. Electrochem. Soc. 144 (1997) 1188.
[7] A.K. Padhi, K.S. Nanjundaswamy, C. Masquelier, S. Okada, J.B. Goodenough, J. Electrochem. Soc. 144 (1997) 1609.
[8] J.M. Tarascon, M. Armand, Nature 414 (2001) 359.
[9] A. Yamada, S.C. Chung, K. Hinokuma, J. Electrochem. Soc. 148 (2001) 224.
[10] A.S. Andersson, J.O. Thomas, B. Kalska, L. Haggstroem, Electrochem. Solid-State Lett. 3 (2000) 66.
[11] S.Y. Chung, Y.M. Chiang, Electrochem. Solid-State Lett. 6 (2003) 278.
[12] P.P. Prosini, M. Carewska, S. Scaccia, P. Wisniewski, M. Pasquali, Electrochim. Acta 48 (2003) 4205.
[13] G. Arnold, J. Garche, R. Hemmer, S. Ströbele, C. Vogler, M. Wohlfahrt-Mehrens, J. Power Sources 119–121 (2003) 247.
[14] H. Gabrisch, J.D. Wilcox, M.M. Doeff, Electrochem. Solid-State Lett. 9 (2006) 360.
[15] N. Ravet, Y. Chouinard, J.F. Magnan, S. Besner, M. Gauthier, M. Armand, J. Power Sources 97/98 (2001) 503.
[16] H.T. Chung, S.K. Jang, H.W. Ryu, K.B. Shim, Solid State Commun. 131 (2004) 549.
[17] H. Huang, S.C. Yin, L.F. Nazar, Electrochem. Solid-State Lett. 4 (2001) 170.
[18] Z. Chen, J.R. Dahn, J. Electrochem. Soc. 149 (2002) 1184.
[19] S. Franger, C. Bourbon, F. Le Cras, J. Electrochem. Soc. 151 (2004) 1024.
[20] P.P. Prosini, M. Carewska, S. Scaccia, P. Wisniewski, S. Passerini, M. Pasquali, J. Electrochem. Soc. 149 (2002) 886.
[21] S.Y. Chung, J.T. Bloking, Y.M. Chiang, Nat. Mater. 1 (2002) 123.
[22] First world congress on microwave processing, in: D.E. Clark, W.H. Sutton, D.A. Lewis (Eds.), Microwave: Theory and Application in Materials Processing IV, The American Ceramic Society, U.S.A., 1997, pp. 7–24.
[23] M.S. Song, Y.M. Kang, J.H. Kim, H.S. Kim, D.Y. Kim, H.S. Kwon, J.Y. Lee, J. Power Sources 166 (2007) 260.
[24] P.S. Herle, B. Ellis, N. Coombs, L.F. Nazar, Nat. Mater. 3 (2004) 147.
[25] A.C. Larson, R.B. Von Dreele, Los Alamos National Laboratory Report LAUR, 86, 1994.
[26] M. Nakayama, K. Watanabe, H. Ikuta, Y. Uchimoto, M. Wakihara, Solid State Ionics 164 (2003) 35.
[27] Y. Xu, Y. Lu, L. Yan, Z. Yang, R. Yang, J. Power Sources 160 (2006) 570.
[28] T.C. Gibb, Principles of Mössbauer Spectroscopy, John Willey & Sons, U.S.A., 1976, pp. 73–101.

[29] A.S. Andersson, B. Kalska, L. Häggström, J.O. Thomas, Solid State Ionics 130 (2000) 41.
[30] M. Sainful Islam, D.J. Driscoll, C.A.J. Fisher, P.R. Slater, Chem. Mater. 17 (2005) 5085.
[31] R.G. Tissot, M.A. Rodriguez, D.L. Sipola, J.A. Voigt, Powder Diffr. 16 (2001) 92.
[32] B.D. Cullity, Elements of X-ray Diffraction, 2nd ed., Addison–Wesley, U.S.A., 1978, pp. 324–349.